A hybrid rugosity mesostructure (HRM) for rendering fine haptic detail

Víctor Theoktisto [1] Marta Fairén Isabel Navazo

Departament de Llenguatges i Sistemes Informàtics
Universitat Politècnica de Catalunya, Barcelona, Spain

Abstract

The haptic rendering of surface mesostructure (fine relief features) in dense triangle meshes requires special structures, equipment, and high sampling rates for detailed perception of rugged models. Some approaches simulate haptic texture at a lower processing cost, but at the expense of fidelity of perception. We propose a better method for rendering fine surface detail by using image-based Hybrid Rugosity Mesostructures (HRMs), composed of paired maps of piece-wise heightfield displacements and corresponding normals, which are layered on top of a less complex mesh, adding greater surface detail than the one actually present in the geometry. The core of the algorithm renders surface features by modulating the haptic probe's force response using a blended HRM coat. The proposed method solves typical problems arising at edge crossings, concave foldings and smoothing texture stitching transitions across edges. By establishing a common set of specially devised meshes, HRM mesostructures, and a battery of performance tests, we build a usability testing framework that allows a fair and balanced experimental procedure for comparing haptic rendering approaches. The trial results and user testing evaluations show the goodness of the proposed HRM technique in the accurate rendering of high 3D surface detail at low processing costs, deriving useful modeling and perception thresholds for this technique.

Key words: Haptic Rendering; Mesostructure; Displacement mapping

1 Introduction

Haptic systems provide unique and bidirectional communication channels between humans and virtual environments in a manner much closer to personal physical manipulation. Haptic interfaces enable direct interaction with computer-generated objects, and when coupled with an intuitive visual display of complex data raise applications to new levels; these applications include molecular docking, nanomaterials manipulation, surgical training, virtual prototyping, machine assembly and digital sculpting.

Email address: {vtheok, mfairen, isabel}@lsi.upc.edu (Isabel Navazo).
[1] On leave from Universidad Simón Bolívar, Caracas, Venezuela

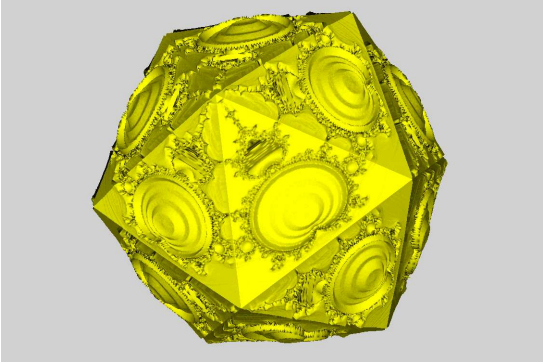

Fig. 1. Sensing a mesostructure coat placed on top of a regular mesh

Haptics drives the development of new algorithms for object's volume and surface modeling, volume processing, and the visualization of novel data structures able to encode shape and material properties. From single one-point based, single person operation to multi-point, multi-hand, and multi-person interaction scenarios, its enticingly rich interactivity is within reach of many computer graphics applications.

One of the interesting applications of haptic perception is to be able to feel, thorough a haptic device, variations in texture, roughness and detail of the surface being contacted. Although some research has been oriented in this direction, there is no contrasting study comparing results of applying different techniques to the same models and textures. We surmise that algorithms that rely solely on a dense geometric representation for haptic collision detection may actually degrade accurate perception because of inherently decreasing sampling rates. The general idea, as in visualization, would be to keep sampling rates high by simulating roughness and other surface features without increasing the geometric density of the model

In this research, we describe our solution for haptic rendering of both high frequency and low frequency detail, allowing a complete perception ranging from fine surface texture to major topographic features. We analyze its advantages and disadvantages against other haptic rendering techniques. Our main contributions are:

(i) A specific model and algorithm for rendering image-based mesostructure surface details mapping paired displacement and normal maps onto underlying simplified geometries (Algorithm 2 in section 4);
(ii) A blending function for smoothing height/normal computation at folding edges (in subsection 4.1) and mesostructure transitions (in subsection 4.2); and
(iii) A battery of usability tests over a chosen set of meshes and mesostructures, allowing the measuring of feature quality perception at varying resolutions (in subsection 5).

We achieve accurate correspondence between the visualization of surface detail and the haptic perception of its fine features, without compromising rendering rates or fidelity of touch.

The article is organized as follows: in section 2 we present related work recently done in haptic rendering. Section 3 describes the approach, its algorithm, suitability, advantages and disadvantages against the two other models. In section 5 we detail the testing protocol for measuring users' perception of haptic properties, describe the testing meshes and trial mesostructures, and summarize the results. Finally we present relevant conclusions and delineate future work towards obtaining a generalized model for highly detailed mesostructure perception in very dense meshes

with very low performance penalty.

2 Related work

The term haptic rendering as defined by Zilles and Salisbury [1] is applied to the realtime computation and generation of force responses to users interactions with virtual objects. Although there has been some work in *pseudo haptics* in simulating surface properties using common computer mice [2], it is more common the use of a specialized haptic interface that exerts a force-feedback response. This resulting force is computed from a combination of forces and torques for a given position and orientation of the interaction device. Users can manually navigate, explore and feel the shape and surface details of virtual objects in the growing field of *computer haptics* [3].

With device sampling rates standardizing in the 1000 Hz range, as in the Phantom or HAPTIC-Master device [4], efficient haptic-interaction techniques may go beyond the simple detection of geometric primitives, towards allowing real-time rendering of arbitrary surfaces of irregular detail, conveying spatial and material properties. All this without forgetting its other role as an user-interaction device for high level event acquisition, recognition of tactile “icons” and general haptic user interfaces or HUIs [5].

When used as an aid for navigating a space, its short range reach requires space exploration strategies, such as a moving bubble for navigation [6], a workspace drift control allowing perception discrepancies between visual and haptic space [7], or a force-filled constraining movement [8]. Collaboration across networks allows simulation of real-time activities such as stretcher-carrying [9], but it brings its own set of latency and simultaneity problems that may cause oscillations in the interaction.

The most simple haptic model uses simple surfaces based on triangles, a point-based device and collisions detection, based on Zilles and Salisbury constraints-based haptic rendering [1]. A haptic cursor representing a force-feedback device is placed into a 3D environment, and a high priority event loop checks whether it collides with the surface of an object, after which it produces a repulsing force of varying direction and magnitude, which physically combines with the force exerted by the user in the haptic device, correcting any penetration ruled out by the object’s geometry [10]. Using a ray-based rendering algorithm with the same setup allows perceiving torque and force-torque feedback mechanisms [11], while using a third object as a extended probe allows also texture differentiation and shape perception [12].

There is also the issue of perceiving several other important physical properties besides geometry. Detecting friction among objects is achieved by rubbing simulated known materials [13] against each other and then computing the expected friction force using common physical models. Surface softness or elasticity may be represented using an array of force pins under a flexible plate [14] or by modeling virtual mass springs at selected mesh points [15]. Forces are mapped to the programmable pin array and the plate bends accordingly when pressed, allowing perception of rubbery or spongy surfaces. In modeling deformable or rupturing 3D medical volumes [16], the haptic probe directly modifies meshed geometries representing soft tissue surfaces, either by point displacement, carving or splitting. All these allow using the haptic device as interaction tool, to explore 3D medical images [17], or as navigational aids for blind users [18].

These efforts choose among several alternatives for modeling and rendering surfaces. Gregory *et all*'s H-Collide [19] uses hybrid hierarchical representation, consisting a hash table of uniform grids and trees of tight-fitting oriented bounding boxes, whereas Johnson [20] uses a pure geometric approach to haptically render arbitrary polygons using neighborhood proximities in order to reduce computational load. Some haptic techniques and approaches are derived from analog visualization techniques, treating the haptic probe as a "contact camera" system. Morgenbesser and Srinivasan in [21] propose the alternative method of *force shading*, with roots in *Phong shading* and *bump-mapping* in visualization. It is defined in this context as modulating force response in the direction of a normal vector sampled from a map. It succeeds in producing sensations of bumpy feelings or vibrations in flat surfaces, but it is unable to elicit accurate geometric perception.

A first effort to measure haptic discrimination of basic 2D textures was the Sandpaper System by Minsky and Lederman [22]. Users manipulated a force-feedback joystick to traverse across screen patches with several sample textures and report qualitative roughness differences. An arbitrary parametric model was used to model the force response. Siira and Pai [23] incorporate an stochastic model of actual physically correct surface properties to produce the appropriate textural feel, including friction and lateral forces. Costa and Cutkosky [24] generate fractal rugosity procedurally on flat surfaces and measure perception thresholds. A model for measuring haptic properties of real surfaces through a point probe is developed by Klatzky and Lederman [25], testing perception quality varying haptic probe spherical radius, traversal speed and exerted force.

A global procedure for mapping a gray-scale image as a displacement map for point-based haptic rendering using standard texture mapping techniques [26] is given by Ho *et al* [27]. It works only for purely convex objects of genus 0 (with no holes), without any assessment of touch effectiveness, sensation fidelity or usability measures. Jagnow [28] modifies mesh surfaces using geometric displacements. Each triangle of a decimated mesh is enclosed in a square slab containing a bilinear patch. Each patch controls a finer submesh that is displaced when the haptic probe presses (or pinches) the bilinear patch. The force, as usual, is exerted in the opposite direction of the slab's normal, appropriately interpolated out of its main vertices. Inadequate modeling or suboptimal rendering produce instabilities in the force responses, as shown in the work of Choi and Tan [29, 30]. It also detects additional effects such as *buzzing* (high frequency resonance vibrations due to first contact) and *aliveness* (perception of surface movement in rigid surfaces). Collisions are detected against a coarse geometry and then against a second microgeometry layer. The problem of incorrect renderings when traversing concave foldings (due to incrustations of adjoining macrogeometries) is identified but not addressed.

A similar approach for painting and sculpting textures onto geometry with a haptic stylus is used by Kim *et al* [31], in which a 2D texture is used to produce geometry changes in the underlying mesh. It also incorporates surface forces such as friction and magnetic attraction to a force shading procedure that strives to keep the haptic probe in contact with the surface.

Potter *et al* [32] provides a simple model to perceive the haptic variation of large heightfield terrains, effecting collisions against bilinear interpolation patches covering a large terrain dataset (a big single-faced object), but does not address objects with many facets. In a different approach, Otaduy *et al* [33] use an object as probe to sample another object's relative friction by averaging the multiple contact areas produced when parameterized isosurfaces collide. Penetration depths are computed from the intersecting isosurfaces, and a repulsing force is computed proportionally

to the highest difference.

For a more thorough understanding of all issues involved in the perception of haptic properties, an extended survey of current haptic rendering techniques can be found in Laycock and Day [34]. It should be noted from the latter review that most haptic rendering approaches on meshes have relied either on straightforward collisions against the mesh's triangles or collisions against a NURBS parameterization of the mesh, with or without force shading. As far as shown, there has been no systematic treatment of the issues surrounding the use of heightfield displacements for haptic rendering, such as concave areas treatment and edge-crossing smoothing. Moreover, there is a lack of a unified testing framework for measuring quantitative and qualitative differences among rendering approaches using perception and usability trials on standard models and surfaces.

In the following sections we develop a new treatment for haptic perception of fine detail, postulating a method that dresses triangle meshes with image-based composite mesostructures "coats", built out of heightfield displacement textures and normal maps. These mesostructure coats are used to create, enhance or substitute surface features in low, mid and higher frequencies, adding non-existent detail at a very low processing cost. We then delve into explaining the set of usability tests that allow us a fair comparison of rendering techniques using the same mesh models and surface details. This allows us to measure quantitative differences on perception, performance, and suitability for surface fine detail, and also to determine the limits in which the proposed solution serves its purpose.

3 Models for haptic perception of surface details

The simulation of surface details in very complex models has not been a problem from the visualization point of view since the late 70's. Algorithms such as the use of colored textures or bump-mapping are well known in the literature [35].

In the case of haptic perception, as we have seen in section 2, any simulation algorithm should be efficient enough to achieve the high frequency updates required by the human sense of touch to perceive a continuous surface.

Our objective is to find an algorithm to allow haptic perception of surface details in objects represented by triangle meshes, and to compare it to other known solutions.

Based on all previous works we can summarize a taxonomy for haptic detail rendering, which determines the particular algorithm to be used.

- *Geometric Detail*, rendering the surface as detailed polygonal meshes (Figs. 2(a) and 2(d)), NURBS, or point clouds, and detecting collisions against the surfaces.
- *Surface Relief Detail*, in which a haptic texture is sampled in lieu of the actual surface. On its own, haptic textures may be based on normal force maps (Figs. 2(b) and 2(e)) or heightfields (Figs. 2(c) and 2(f)).

The *force shading* algorithm [3] uses the normal vector at discretized surface points to calculate the force direction and magnitude to be applied to the haptic device when it collides with the

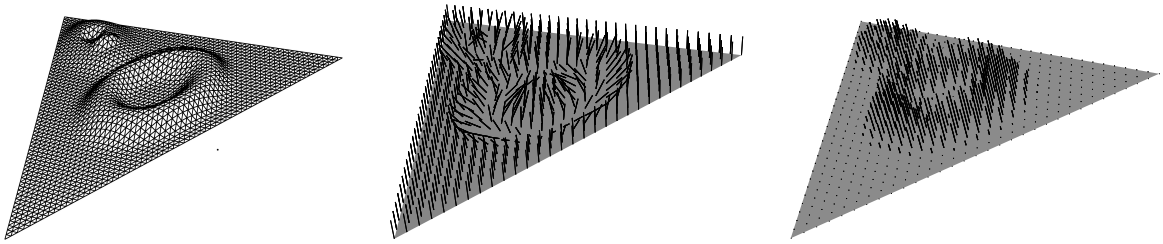

(a) Rings - Geometry (b) Rings - Force shading (c) Rings - Heightfield displacement

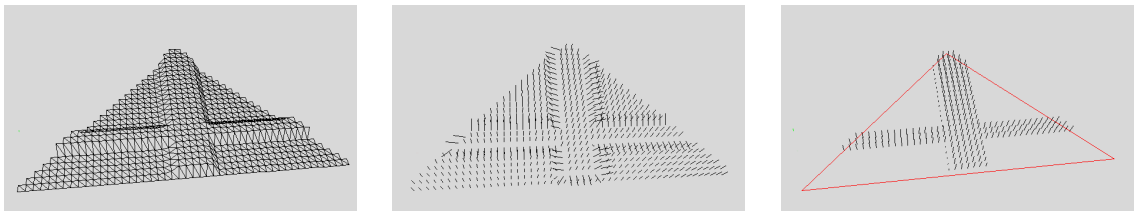

(d) Cross - Geometry (e) Cross - Force shading (f) Cross - Heightfield displacement

Fig. 2. Approaches for simulating surface details in haptic perception

triangle [figures 2(b) and 2(e)]. By using this haptic perception algorithm and implementing its *bump-mapping* visualization as a GPU shader, one can achieve a correct perception of surface roughness for small height differences. Since the collision is always detected against the triangle of the mesh, an upward/downward perception of displacement from the triangle surface is not possible.

We offer below a brief summary of an earlier approach we developed for rendering individual surface detail out of an underlying triangle mesh, by building a constraint-based force response against local heightfield displacements modulating 6 DoF spring/damper objects. The method, shown here as Algorithm 1, compares favorably against a force shading implementation for rendering/perceiving the same models using equivalent normal force maps for texture perception. The complete model and procedure can be found in [36].

The procedure used for this approach worked as follows: A search in 3D space for the exact *probe*'s collision coordinates against some small facet is substituted by a procedure that identifies a collision against a much larger triangle, followed by a 2D mapping/search of the haptic probe's position into the closest surface detail in that triangle. The algorithm starts by determining, quickly and at a low computational cost, the base triangle being *potentially* collided by the haptic probe, giving the haptic render algorithm ample time to sample the appropriate heightfield altitude, determine whether there is an actual collision point (the haptic interaction probe is below that height), and if that is the case, exert the appropriate repulsing force using penalty-based force computation model.

A bounded prism is created for each mesh base triangle $T_k = \langle V_{k,0}, V_{k,1}, V_{k,2} \rangle$, with equal displacements up and down a maximum distance *mh* along each vertex normal, containing all possible heightfield values (see figure 3(a)). The 8 triangles thus created (2 for each of the 3 quadrilateral sides, plus the top and bottom triangular lids) share the same tagging label of the original base

Algorithm 1 Haptic heightfield-displacement rendering

loop
  Sample haptic probe position $P_H = (x_H, y_H, z_H)$;
  Detect potential collision with a triangle in the mesh;
  if ($\exists$ collision with some triangle prism T) **then**
    {*haptic probe P_H is inside T's prism*}
    Project P_H against T obtaining surface point P;
    Compute 2D texture coords (s,t) of P over T;
    Sample the heightfield displacement $Z = H(s,t)$;
    if ($penetration = Z - distance(P_H, P) > 0$) **then**
      {*Positive penetration, a real collision*}
      Calculate force $F(penetration)$;
      Apply F in the normal $\overrightarrow{N}$ of T at the device;
    end if
  end if
end loop

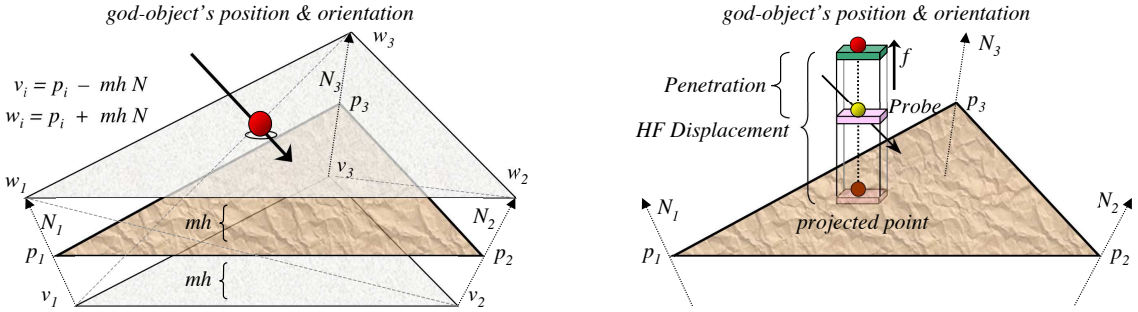

(a) Triangle prism collision area

(b) Collision point computation

Fig. 3. Heightfield collision mapping

triangle, so the identification of the relevant mesh triangle is immediate after hitting any side of the prism.

As shown in Algorithm 1, any collision against a prism's face triggers the haptic rendering of a corresponding heightfield surface displacement map. If at any time the probe elevation's from the triangle descends within the computed height at that point, a repelling force is applied to the haptic probe along the face normal at the projected point, proportional to the height difference (or penetration). This forces the god-object (a constrained proxy of the haptic probe) to continually move towards the surface, at which point the force ceases to be (see figure 3(b)). The haptic probe and the god-object are kept in sync when allowed by the constraint system.

Heightfield displacements were contrived to have altitude zero on the edges of the base triangle mesh to insure C^0-continuity on the edges. This avoids the problem of having extreme height jumps at the triangles' edge. In the case of convex folds, simple normal interpolation may avoid possible instabilities when cruising near the edges, but this was shown inadequate for smooth transitions when sizable height differences exist across face boundaries, and totally wrong for holes and concave folds.

4 Mesostructure model for haptic rendering

We proceed now to elaborate on a method that proposes a global solution to the afore mentioned problems. Instead of applying the force in the normal direction of the base triangle T_k, a much more accurate rendering approach is applying the repulsing force in the exact direction of the normal at the specific impacted surface point. In [33] an approximate normal is computed from the penetration gradient, which depends on the applied force, torque and current probe 6-DoF State. In our present approach we precompute normals directly from the heightfield displacement texture and store it as a normal map texture, creating what we call a Hybrid Rugosity Mesostructure or *HRM*.

Taking into account the traversal direction when touching a surface, the haptic point is pushed in the direction of the normal, and a constraint system combines this repulsion with the force exerted by the user at the probe, producing a change of position and orientation. It is by using heightfields in haptic rendering that the perception of displacement over the base triangle can be achieved. In that manner, we enable accurate haptic rendering without incurring lagged responses or precision reductions. This allows to vary surface sensation exploration by "coating" or "dressing" a mesh and render it with several surface frequencies and reliefs. Therefore, our input data meshes (all but one) are built of similar-sized triangles, to focus on the relief perception part. The exception is a mesh that has triangles of different sizes for exploring the limits of haptic perception.

The general procedure, shown as Algorithm 2, uses the already explained prisms, with an added twist. The HRM of normal and heightfield displacement tuples = $[\overrightarrow{N}(s,t), H(s,t)]$ correspond to one or more RGB-α textures, with the normal $\overrightarrow{N}(s,t) = \langle N_x, N_y, N_z \rangle$ having the $\langle r, g, b \rangle$ coordinates, and the heightfield displacement value $H(s,t)$ having the $\langle \alpha \rangle$ transparency coordinate. The heightfield-normal tuples may be provided as static or procedural 2D, 3D or 4D (+ time) textures, allowing for an even greater complexity of haptic perception. The visual part is rendered by mapping the displacements using the same heightfield and normals, so there is complete correspondence between the haptic and visual renderers. Friction, viscosity, magnetism and other surface properties may be easily added and sampled as additional entries on the HRM structure, requiring only the modification of the force-response accordingly.

Haptic resolution gets scaled in sync with the current visual zoom state. Getting closer to the tested object resizes the haptic space accordingly, so altitudes that perhaps were not measurable at lower zoom levels ("blurred") become distinct and perceivable at higher resolutions, and the touch perception of surface change becomes more accurate.

4.1 Blending haptic mesostructure at the edges

The presented Algorithm 2 computes soft transitions at triangle edges with different mesostructures using a simple interpolation scheme. For each face in the mesh, we keep track of neighborhood information of all adjoining face indices. Two faces are adjoining if they share at least one vertex in common. Neighborhood information is factored in when loading the mesh. Since we are testing low-density meshes made of similar-sized triangles, this means that most vertices are shared between three to six faces. When following along the surface of the mesh, the mesostructures in a neighboring faces may produce an abrupt topographic change at the edge, that if left to

Algorithm 2 Haptic mesostructure-blended rendering

loop
  Sample haptic probe position $P_H = (x_H, y_H, z_H)$;
  Detect potential collision with a triangle in the octree;
  if ($\exists$ collision with some triangle prism T) **then**
    {*The haptic probe is inside the prism*}
    Project P_H against T obtaining surface point P;
    Compute 2D texture coords (s,t) of P over T;
    Obtain α, β, and γ barycentric coordinates of P in T;
    if ($\exists \alpha, \beta$, or $\gamma \geq 1-\rho$) **then**
      {*We are within* ρ *distance of an edge*}
      $AD \leftarrow AW \leftarrow 0$; $\overrightarrow{AN} \leftarrow \overrightarrow{0}$;
      for all adjoining triangles f_i of T (T included) **do**
        Project P_H against f_i to obtain surface point P_i;
        Compute 2D tx coords (u_i, v_i) of P_i over f_i;
        Sample HRM pair $[\overrightarrow{N_i}(u_i,v_i), H_i(u_i,v_i)]$;
        Evaluate weight function ω_i from P, P_i and ρ;
        $AD \leftarrow AD + \omega_i H_i(u_i,v_i)\cdot$;
        $\overrightarrow{AN} \leftarrow \overrightarrow{AN} + \omega_i \overrightarrow{N_i}(u_i,v_i)$;
        $AW \leftarrow AW + \omega_i$;
      end for
      $AD \leftarrow AD/AW$;
      $\overrightarrow{AN} \leftarrow \overrightarrow{AN}/AW$;
    else {*Collision against a single face*}
      Sample HRM pair $[\overrightarrow{N}(s,t), H(s,t)]$;
      $AD \leftarrow H(s,t)$;
      $\overrightarrow{AN} \leftarrow \overrightarrow{N}(s,t)$;
    end if
    if ($penetration = AD - distance(P_H, P) > 0$) **then**
      {*Positive penetration, a real collision*}
      Calculate force magnitude $F(penetration)$;
      Apply F in the normal $\overrightarrow{AN}$ at the device;
    end if
  end if
end loop

stand will produce a sudden force change (in magnitude and orientation) in the haptic device. To eliminate these abrupt jumps, we follow the following stitching procedure to blend the transition among faces.

Heightfield and normals closer to the edges are sampled and interpolated using a multi-texturing approach from the rugosity mesostructure. In Figure 4(a) we see a schematic of this heightfield stitching. A band of parametric size ρ extends at both sides of each edge. In this area we use an alpha-blending function to combine overlapping positions, heights and normals. This function may express any linear or nonlinear blending. We extend each parametric distance of the triangle's barycentric coordinates in this quantity ρ, say 0.05 (or 5%) over each HRM. One of the blending maps of Figure 4(b) is used then to compute an averaged mesostructure that spans parametrically this ρ across each edge.

If the projected point of the haptic probe is inside the ρ band of triangle A (in Figure 4(a)), it

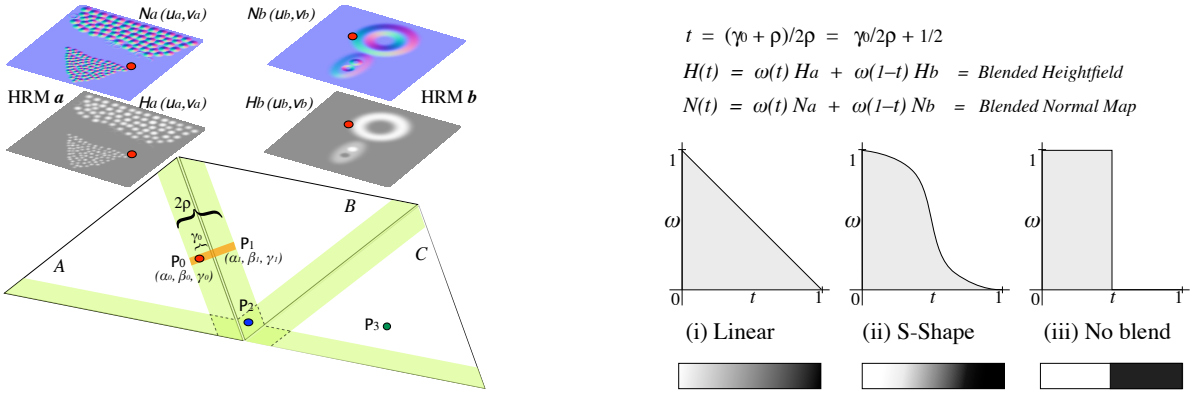

(a) HRM stitching computation

(b) Edge blending functions

Fig. 4. Blending of textures in neighboring triangles

means that at least one of the barycentric coordinates of P_0 is less than ρ at some edge. This point is remapped into the opposing triangle B, obtaining its local set of barycentric coordinates P_1. To blend both heights and normals, we compute a t value between 0 and 1 out of P_0, P_1 and ρ for the chosen blending function, and obtain the corresponding weights $\omega(t)$. Several blending functions may be defined for different effects. For example, if we desire no blending at all, a half white/half black map (Figure 4(b), No blend) will produce the same abrupt relief transition at the edges, generating jumps at edge crossings. A linear gradation from white to black (Figure 4(b), Linear) or sloping S-shaped curves (Figure 4(b), S-Shape) offer more stable and pleasant results. We use the ω weights to compute an average height and normal direction. In the case of point P_2, some additional barycentric coordinate is also less than ρ, so this process is repeated for this adjacent edge. Point P_3 falls outside of the ρ bands, so it is sampled only once.

The approach also holds for convex folds in meshes. When a potential collision is detected against a face, the haptic probe position is tested against the face. If the projected point's barycentric coordinates $P(\alpha, \beta, \gamma)$ has at least one of its values within the ρ band across some edge, a search is initiated, successively projecting against each adjoining face and sampling in the corresponding mesostructure, weighting and averaging all quantities with the corresponding blending values. The *god-object* will be constrained by the added restrictions and move accordingly. The added checking time is negligible when compared to the time taken to find the first collision, and the additional samplings will occur only if close to an edge.

4.2 Haptic rendering in concave faces

A problem that has not been mentioned before is the perception and performance issues of rendering non-convex objects (see figure 5). When two or more triangles form a concave fold or depression (angle between faces less than 180°) the haptic probe can be inside two (or more) prisms at the same time. Basically, the treatment of concave faces is the same applied to flat and convex faces. It will blend heights and normals in a band of size 2ρ around the edges (half in one face, half on the other), so the effect will be a repulsion away from the edge. Unfortunately, this may create a back-and-forth effect at the probe (see Figure 5), sometimes getting stuck and unable to leave the surface, or in rare cases, generating a resonance situation with ever increasing force magnitude, generating a device failure.

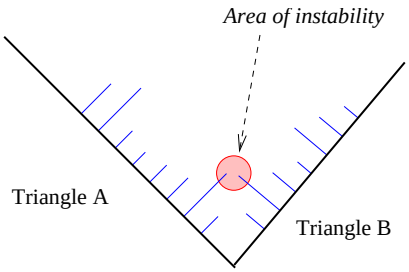

Fig. 5. Possible case of instability

Our solution, having a constant object geometry, is to transform the initial mesostructure texture, so that height and cumulative normals are already mapped for those surface points that collide into other faces, saving the inclusion and collision tests altogether. In Figure 6(a) we see two adjoining triangles and their corresponding unblended mesostructures (blue and yellow), with a subsurface hole (and potential device trap) laying in the middle. At Figure 6(b) we see the result of the blended joint mesostructure, with the hole eliminated. The net effect of the mesostructure preblending is that now the probe is pushed away from the edge in the combined normal direction.

To avoid borderline cases, we add a small ε to the collided heights to avoid getting trapped in a narrow crevice or hole. The probe is detected inside the common region by a simple inclusion test, which can be computed from the current folding angle and each face's maximum heightfield. By precalculating these changes and replacing them back into the mesostructure, the relevant heightfields (red) now reflect the modified surface relief close to the edges (see figure 6(c)).

This approach may be used for stitching different mesostructures at triangle boundaries if so desired. Computing heightfield normals on-the-fly from the heightfield itself is always slower than a single sampling access, so we save some time by precomputing normals using the hybrid model, allowing for better haptic sampling rates. The added complexity resides on the height differences arising from stitching discontinuous HRMs in test meshes. When the HRMs are precomputed from existing fine geometric detail, abrupt height and normal differences are greatly minimized across edges, thus greatly reducing haptic artifacts.

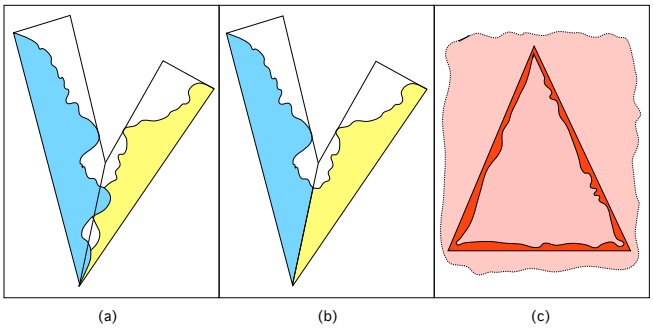

Fig. 6. Precomputed mesostructure mapping

If this seems overly complex and no mesostructure preprocessing is possible, or if the object's mesh geometry is subjected to deformations, the feature blending may also be computed in place, at some performance cost. When the probe is detected within a prism, it may be tested for inclusion against *all* neighboring prisms. Mesostructure blending will occur when the probe approaches the 2ρ band around any edge (see Figure 4(b)). However, the added complications of acute foldings or crevices with sizable height values near the edge (as illustrated in Figure 5) will remain, as will the possibility of getting trapped in a surface hole. Nevertheless, repeated

occurrences of this phenomenon is a sure sign that the underlying mesh could use more triangle detail. This proximity effect is directly proportional to the maximum height value and closeness to an edge. Lower overall heightfield magnitude produces better adjusted behavior and allow for much acuter angles among faces before instability sets in.

5 Results

In order to measure quantitatively and qualitatively participants' ability to perceive each surface's haptic properties, we devised the following protocol for testing choice meshes and haptic textures, using both force shading and HRMs, under the same environmental conditions for each run.

5.1 Testing Method

5.1.1 Equipment

A HAPTICMaster from FCS, having a built-in wide haptic 3D space, able to exert forces from a delicate 0.01 N up to a very heavy 250 N, with a wide 3D perception field, equivalent to a cylindrical wedge of 40 cm x 36 cm x 1 radian. The PC is a 2 GHz Pentium IV with an ATI Radeon 9700 graphics card.

5.1.2 Participants

Each test involved 18 different user tester/trials (6 participants, 3 trials each) for the corresponding setup. Testers were not told beforehand what to expect and were individually tested. All of them had used the haptic device before, and were instructed only to maintain constant force and speed throughout each experiment. Their impressions of quality perception were recorded according to the same live questionary.

5.1.3 Stimuli

We carefully prepared a set of base meshes, shown on Table 1, each one having some uniform geometric properties. To create the set of HRM coats shown on Table 2, we generated the appropriate heightfield displacement maps, and calculated their corresponding normal maps as explained in [37], (which are also used in force shading). In the latter manner we can dress the same mesh with chosen HRM coats representing particular 3D mesostructures. Bi-linear, bi-cubic and other filters may be applied to the textures if smoother surfaces are desired. Each generated HRM exhibits some measurable perception property, either on the space or temporal axis. Although a color texture may be added to the HRM structure, it is irrelevant as a surface haptic property.

5.1.4 Experimental Procedure

A total of 5 separate experiments were performed on the participants.

I *Baseline perception:*
A control setup, so users recognize what a featureless surface feels like.

II *Differences in sensation perception:*
Testing visual-haptic perception quality differences of abrupt, sloping or bumpy surfaces.

III *Perception of mesostructure with simple repeating patterns:*
Testing perception of equally spaced ridges and grooves.

IV *Perception of non-monotonous mesostructure:*
Testing ability to perceive definite shapes in non-monotonous haptic textures.

V *Perception of visual-haptic disparity in a gradated mesh:*
Testing changes in visual-haptic perception at changing resolutions.

Each test session consisted in a different $\langle Mesh, HRM, Test \rangle$ triad being executed. The experiments (shown on Table 3) were performed and measured modulating the maximum amplitude of heightfield displacements, at 1%, 5%, 10%, 15% and 20% of the average edge length of each mesh. This proved a better predictor than some factor based on average triangle mesh area, since it does not produce rendering artifacts in close to degenerate triangles.

Table 1
Trial model meshes

Mesh	*Description*
M_a	Open regular mesh (flat surface of near equilateral triangles).
M_b	The same mesh as a softly convex surface (folding angles in [180°, 225°].
M_c	Similar to M_b, but faces fold at acute, square and obtuse angles.
$M_{d,j}$	Closed convex meshes (spheres), beginning with an Icosahedron.
M_e	Open concave regular mesh in the shape of a “cup”.
M_f	Open mesh of a regular gradation of triangles, from big to small.
M_G	A much denser mesh based on M_b, with very small triangles following the heightfield instead.

Table 2
Trial hybrid rugosity mesostructures

HRM	*HRM feature description*
H_0, N_0	A uniformly flat surface, to be used as the baseline.
$H_{1,k}, N_{1,k}$	A family of serrated patterns (steep vertical left side; sloping right side), of increasing frequency in k.
H_2, N_2	Raised beams crossing at right angles.
H_3, N_3	Gently sloping rings, peaks and holes.
H_4, N_4	Bumps and warts of varying sizes and densities.
H_5, N_5	Raised flat cylinders (like a coin).
H_6, N_6	Grooved or engraved letter *S* (a *negative* heightfield).
H_7, N_7	A fractal mountain range, with peaks and valleys.

Table 3
Trial tests protocol

Test Description	*Model*	*HRM*	*What is measuring*
I.- Baseline perception of null mesostructure.	*All*	H_0	*Perception of edge crossings.*
II.- Perception of visual-haptic sensation quality	M_a, $M_{d,j}$	H_2, H_3, H_4	*Perception differences between haptic rendering algorithms.*
III.- Perception of monotonous mesostructure (simple pattern).	M_a, M_b	$H_{1,k}$	*Visual-haptic resolution calibration, height variation, feature counting, groove orientation.*
IV.- Perception of non-monotonous mesostructure (complex patterns).	M_b	H_2, H_3, H_4 H_5, H_6, H_7	*Visual-haptic correspondence, height variation, contour following, bumpy quality.*
V.- Perception of visual-haptic resolution disparity of mesostructures in a gradated mesh	M_f	H_1, H_2, H_3	*Limits of feature perception.*

5.2 Test I. Baseline perception

The baseline perception was designed so testers would find no differences between a simple collision with the underlying mesh geometry, and the same geometry with the flat mesostructure H_0 (a constant height of zero throughout).

5.2.1 Evaluation of results

With respect to mesh M_a (flat mesh of equal triangles) and M_f (flat mesh of unequal triangles) all testers detected no edge crossings or features whatsoever. Working with meshes M_b and M_d, they detected edge crossings only when such edges were among faces joining at non-flat angles. As expected, there was no spurious detection of any other surface feature in both rendering approaches.

5.3 Test II. Differences in sensation perception

For this test, we chose a sphere as the base model, built recursively at several resolutions. To better appreciate the rendered surface texture in the figures appearing in this article, it has been set to the simplest possible resolution, a perfect icosahedron).

Afterward, we generated synthetic HRMs, and used them to compute the corresponding normal maps. In this way we obtained the corresponding pairs of heightfield and normal maps shown on Figure 7. In the end we settled for the three textures shown here, since each allows perception of different surface characteristics.

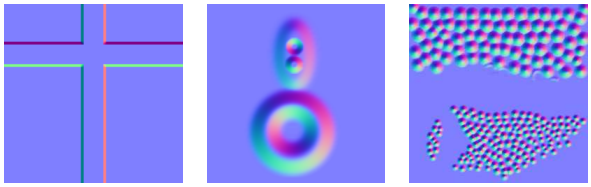

(a) N_2 N-map (cross) (b) N_3 N-map (ovals) (c) N_4 N-map (warts)

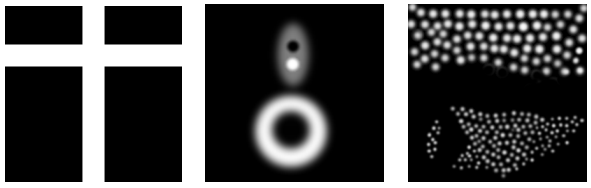

(d) H_2 H-field (cross) (e) H_3 H-field (ovals) (f) H_4 H-field (warts)

Fig. 7. Normals and Heights maps

The chosen textures were: one with alternating polished and variable bumpy areas (N_4 and H_4), one with gently sloping circles within a soft gradient (N_3 and H_3), and one with an embossed cross having only horizontal and vertical surfaces (N_2 and H_2). Additionally, taking advantage of the graphics card hardware, we implemented the shader part corresponding to our force shading in the GPU, just to allow a better haptic sampling rate.

5.3.1 Evaluation of results

We show on figure 8, different renderings using force shading and HRMs. It is evident from the figures that normals in bump mapping/force shading make for a smoother visualization. However, in terms of haptic perception, the comparisons are quite different and depend on the characteristics of the texture map.

We compared the haptic perception of the user in both methods, force shading and our heightfield algorithm, with several texture maps with different characteristics, as described next:

- In the case of a displacement map such as the one shown in figures 8(e) and 8(f), where the texture image shows two bumpy areas, the resulting perception is somehow similar in both methods. The user perceives a certain roughness in the fine bumpy area and a bumping feeling and certain guidance among bumps in the coarse bumpy area.
- In the case of a displacement map such as the one shown in figures 8(c) and 8(d), where the texture image shows a big oval and two small bumps over the surface, the resulting perception is a bit different between the two methods. In the part of small bumps there is almost no difference, but in the big oval part, when the user is inside the oval, although in both cases there is some similar resistance to go out, with the force shading method the user only perceives the resistance for going up to the oval while with the heightfield method the perception is clearly going up to the oval and down from it.
- In the case of a texture shown in figures 8(a) and 8(b), where the texture image shows a cross

step over the surface, the perception is clearly different between the two methods. With the force shading method the user only perceives resistance on the going up and a jump going down, but no height differences can be perceived. With the HRM method the user perception is clearly better in this case, because the parts of the cross going up and down give the feeling of going up and down with different height on the top of the cross than on the base.

As a summary for this comparison, we can conclude that the force shading method can be a good approximation for modeling an apparent roughness of material, but is not sufficient for irregular normal maps where the perception has to be tight to the texture shape we want to simulate. This problem is solved with our HRM algorithm, which gives an accurate sense of the surface characteristics.

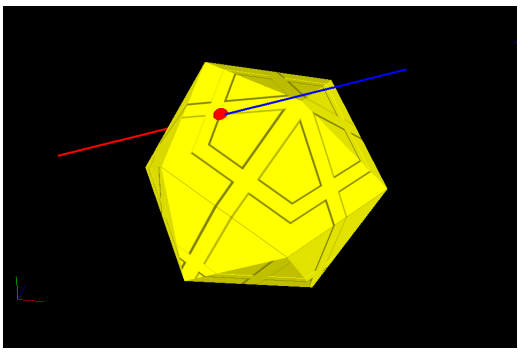

(a) Cross (using force shading with N_2)

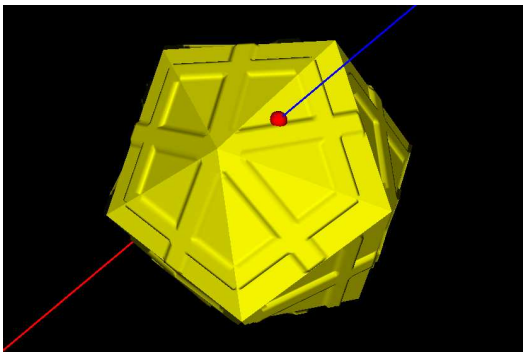

(b) Cross (using HRM H_2, N_2)

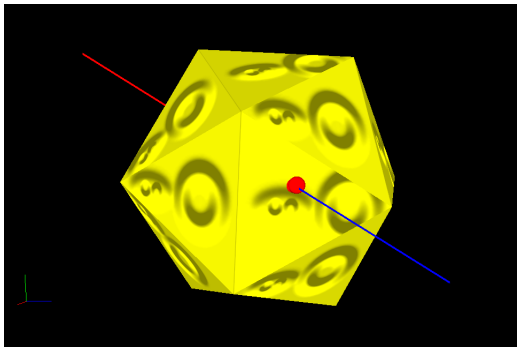

(c) Ovals (using force shading with N_3)

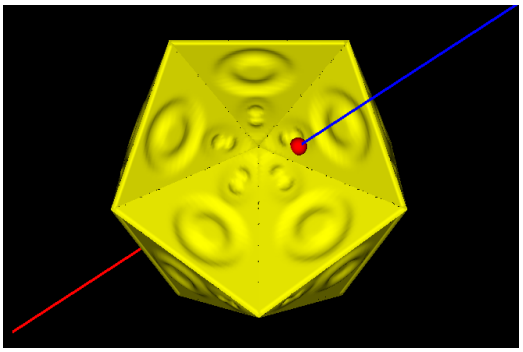

(d) Ovals (using HRM H_3, N_3)

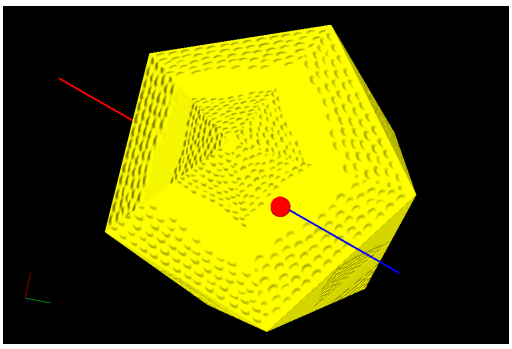

(e) Warts (using force shading with N_4)

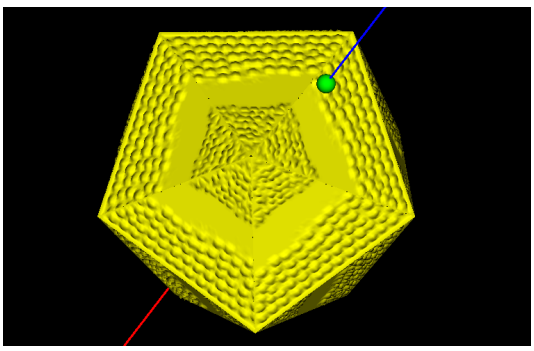

(f) Warts (using HRM H_4, N_4)

Fig. 8. Haptic perception: Force Shading vs. HRM

5.4 *Test III. Perception of mesostructure with simple repeating patterns*

This test was devised to test the lower and upper limits of haptic modeling and perception using the HRM approach. We chose a simple repeating texture in a regular serrated pattern, each ridge with a left vertical side and a sloping right one. The test measures several perception variables related to haptic resolution: How far are they spaced? Can the ridges be counted? How does it feel when going left-to-right and back?. Each trial was performed on the base mesh M_b using HRMs $H_{1,j}$ with the same serrated pattern at different resolutions (and corresponding precomputed normals $N_{1,j}$, see figures 9(a) and 9(b)).

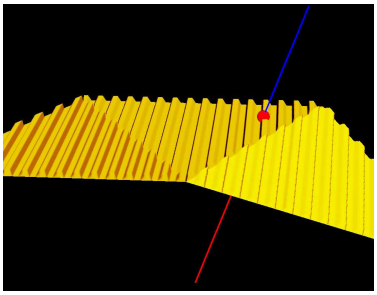

(a) Coarse serrated HRM $H_{1,32}, N_{1,32}$

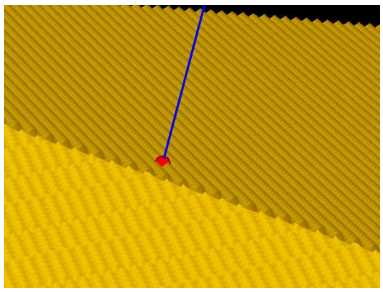

(b) Fine serrated HRM $H_{1,512}, N_{1,512}$

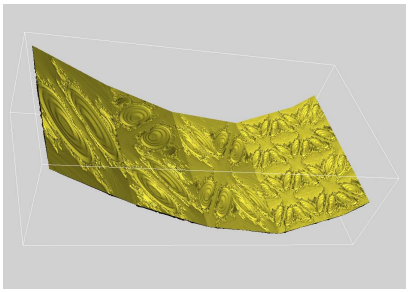

(c) Concave mesh M_f with HRM H_7, N_7

Fig. 9. Perception scaling adjustment for mesostructure

For each trial, the maximum heightfield value (that is, the altitude of the prism) was modulated at 1%, 5%, 10%, 15% and 20% of the average length of the mesh' edges, and run in trials with several users. It is to be noted that force shading failed miserably this test, detecting just undirectional vibration at higher frequencies and shown to be unreliable at best at lower ones.

5.4.1 *Evaluation of results*

When we tested the HRMs, ranging the surface frequencies from few ridges to many, only the last two showed a performance threshold. *Frec256* is a mesostructure that has an asymmetric serrated peak-valley combination repeated 256 times, and *Frec512* is correspondingly doubled. Each were tested up to at a corresponding visual resolution of 1 pixel wide for each ridge. The results hint to a practical limit on how much geometry variation may be modeled and perceived by the

mesostructure approach. Higher than that is an indication that more triangles and recalculated mesostructures are needed to better represent surface haptic details. The results are summarized in figure 10(a) and figure 10(b):

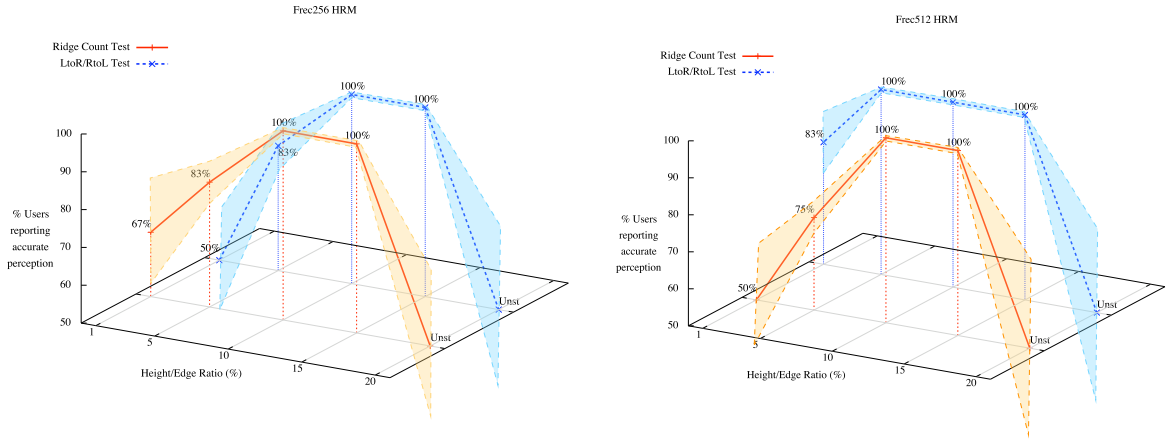

(a) Test results for Frec256 HRM $H_{1,256}, N_{1,256}$ (b) Test results for Frec512 HRM $H_{1,512}, N_{1,512}$

Fig. 10. Haptic perception of heightfield textures

The solid line in each graph represent the test sample mean and the surrounding shaded areas represent an amplitude of two standard deviations around each value. Three important experimental facts that can be extracted from this results:

- There exists a definite region for the best perception of haptic features, which sits between maximum peaks and valleys of 5%-15% of a triangle's edge size, with a "sweet spot" with optimum perception at prism altitude 10%. The 5%-15% region holds also for dynamic characteristics, such as sense of direction in the grooves, and sensing the difference between going left-to-right or right-to-left as abrupt or sloping. However, at the highest texture resolution, all test subjects only felt vibration without discerning any sense direction or damping. This is reflected on the standard deviation intervals around each plot. The deviation drops to zero in the 5%-15% region (All testers reported accurate perception of surface features), but results diverge at the ends of the scale.
- At small height differences, the variability in the perception of ridges and direction by testers is to be expected, since faint features are not perceived by everyone.
- Height modulations greater than 20% resulted in growing instabilities in the haptic device, due to wild and fast changes in the normal direction because of continuing exerted forces in high vertical walls, and overshooting of features due to feedback kick. This also caused the variability at the other end of the plot.

These results hint at a practical threshold on how much geometric mesostructure may be modeled by this approach. In one end of the variation scale, mesh zones where surface variation exceeds 15% of average edge size are thus candidates for finer remeshing. In the other end of the scale, if a triangle is perceived as less detailed as the haptic texture dictates, the haptic sensation may be enhanced by using the same texture sampled at a lower rate.

On the other hand, high resolution mesostructures with below-the-threshold heights become perceptible when zooming on the scene (see figure 11). The scaling effect is kept in sync between

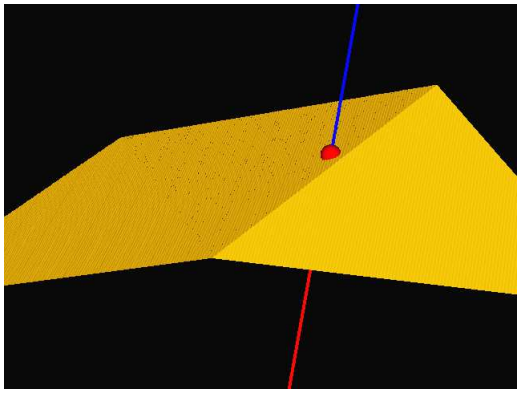

(a) High resolution mesostructure from afar

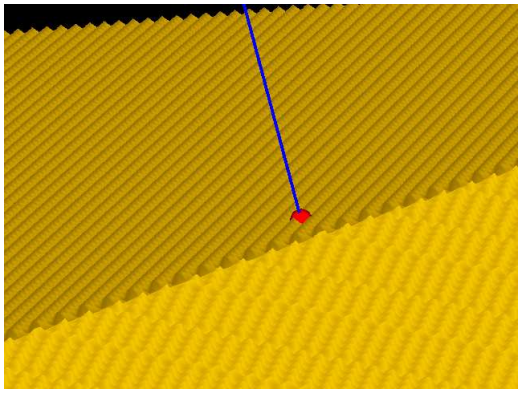

(b) High resolution mesostructure up close

Fig. 11. Perception scaling adjustment for mesostructure

the visual and haptic field of view, so sensation becomes increasingly defined when going from afar (figure 11(a)) to near (figure 11(b)). The size of the haptic probe is correspondingly reduced so it follows much more accurately the valleys and ridges in the texture. The reverse is also true, when going the other way, features become less perceptible.

5.5 Test IV. Perception of non-monotonous mesostructure

In this test we measure the ability to perceive definite shapes in the haptic textures: A hard-edged cross; a soft texture of sloping rings, peaks and depressions; small-to-big warts or bumps; a protruding feature in the shape of a coin; a groove in the shape of the letter S (see figure 12). The object of this test is the multi-modal quality of perception: how much it corresponds with the visual representation and whether can be “followed along”.

5.5.1 Evaluation of results

As can be extracted from the table, event small scratches are felt and followed, until they become too deep and narrow for a proper rendering of the haptic forces generated. All testers were able to accurately detect the target features even a low resolutions, so there is no variance worth reporting, except when reaching the 20% threshold level, at which point instability sets in and perception degrades quickly.

5.6 Test V. Perception of visual-haptic disparity in a gradated mesh

Here we measured resolution changes in perception. We map the same haptic texture into a mesh (M_f) made of rectangular triangles of decreasing size, in order to test the limits of perception, aliasing effects and arising instabilities. We also measure how these qualities change as we zoom (both haptically and visually) in the mesh.

Table 4
Haptic perception of fine features in non-monotonous mesostructure

% Height	**1%**	**5%**	**10%**	**15%**	**20%**
Straight walls	100% yes	100% yes	100% yes	100% yes	unst
Round contours	100% yes	100% yes	100% yes	100% yes	unst
Grooves	100% yes	100% yes	100% yes	100% yes	unst.
Soft slopes	100% yes	100% yes	100% yes	100% yes	100% yes
Small bumps	100% yes	100% yes	100% yes	100% yes	83% yes 17% no

5.6.1 Evaluation of results

In trial mesh M_f (Figure 9(c)), neighboring triangles progressively reduce their area in half from left to right (height is reduced by $sqrt(2)/2$). Since mesostructure remains at the same resolution, the resulting mapped areas actually double their density from left to right, and sampling aliasing occurs. Sharp features perceptible at big triangles become smoothed at smaller triangles. If the scene is zoomed in (or out) they become sharper (or smoother) again. A feature becomes undetectable when the height difference becomes less than a corresponding visual pixel, just as expected by the Nyquist limit. In other words, if a visual difference is seen, then it can be felt.

6 Conclusions

We have developed a fast and accurate method for rendering local haptic texture in triangle meshes, which allows the user to perceive correct surface details at several resolutions. This extends the use of height field haptics beyond the usual field of gigantic terrain textures and allows perceiving higher surface detail without modeling them geometrically. This approach can be used for locally mapping relief textures in triangular meshes and haptically render them in real time. The method even allows managing LoD in the visual and haptic resolutions for closer approximations, and we have the added benefit of having a repository of assorted HRMs. Given that all HRMs are functions, a procedural HRM fits without any change in our scheme.

In order to apply our method for perceiving overlayed scratches on the surface [38], we have extended it to accept HRMs having pure negative values, to represent inverse heightfields (see figure 12). In these cases, force shading is not able to give the correct perception because there are neighbor points with very different normals which actually pushes the haptic probe away from the scratch. Our HRM-rendering algorithm allows a correct perception of this sort of characteristics as well, even cruising along the grooves of the scratches.

The approach shows ample suitability for modeling and perceiving in real time very complex

surface textures of varying frequency out of simpler geometric models such as bones, major body organs, machine assembly pieces and other structures.

We are extending further this research by exploring a superposition of multiple resolution haptic textures approaches. This would allow a better perception of heightfield displacements where more haptic detail is needed by simulating further relatively steep slopes or zooming in a high frequency range. Using the results obtained in this research, we are devising a procedure to scan an object's fine geometry from large meshed models of small triangles, and replace it with a less dense mesh of larger triangles that captures all the perceptible surface frequency details of the original model, as a blending continuity of global mesostructure atlases (height displacements, surface normals and other properties such as directed friction and stickiness).

Our model allows adding material friction as a constant global coefficient, or expanding the HRM with a second 2D texture field whose value represents a variable friction coefficient at each triangle point. This will allow to include the added resistance of fine microstructure surface properties into the model. We expect to measure performance differences between using an HRM-based approach against a pure geometric model when rendering haptic collisions, and obtaining a robust answer to that question. The approach uses haptic impostors to replace the nearest object geometry, and in some ways is similar to the visualization algorithm that Policarpo [39] and Baboud [40] describe for fast shading of geometric objects using displaced-mapped impostors, either as an assembly of a two-sided (back/front) map or a six-sided (cube map).

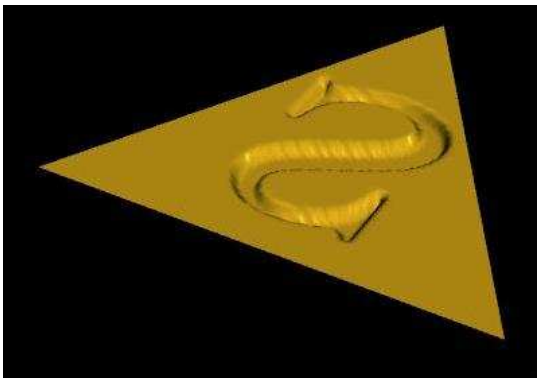

Fig. 12. Example of a negative heightfield

Acknowledgments

We want to thank Iban Lozano for his valuable help on the implementation of shaders. We extend our thanks to Eva Monclús, Santiago Murillo, Antoni Xica, and Marcos Balsa for their observations and patience during the measuring phase.

This work has been partially co-financed by project TIN2004-08065-C02-01 of the Spanish Government (MEC) and FEDER funding, and by project II-021-FA of the UE ALFA Cordial-2 network.

References

[1] C. Zilles, J. Salisbury, A constraint-based god-object method for haptic display, in: Proc. IEEE Int'l Conf. Intelligent Robots and Systems, IEEE Computer Society, Washington, DC, USA, 1995, pp. 31–46.

[2] A. Lécuyer, J.-M. Burkhardt, L. Etienne, Feeling Bumps and Holes without a Haptic Interface: the Perception of Pseudo-Haptic Textures, in: Proceedings of CHI 2004, 2004.

[3] C. Basdogan, M. A. Srinivasan, Haptic rendering in virtual environments, in: K. Stanney (Ed.), Handbook of Virtual Environments, London, Lawrence Earlbaum, Inc., 2002, Ch. 6, pp. 117–1343, 2212–2218.

[4] FCS Control Systems, The Netherlands, HapticMASTER Installation Manual (December 2002).

[5] K. MacLean, M. Enriquez, Perceptual design of haptic icons, in: Proceedings of the Eurohaptics 2003, Dublin, Ireland, 2003.

[6] L. Dominjon, A. Lécuyer, J.-M. Burkhardt, G. Andrade-Barroso, S. Richir, The "Bubble" Technique: Interacting with Large Virtual Environments Using Haptic Devices with Limited Workspace, in: Proceedings of the First Joint Eurohaptics Conference and Symposium on Haptic Interfaces for Virtual Environment and Teleoperator Systems, 2005.

[7] F. Conti, O. Khatib, Spanning large workspaces using small haptic devices, in: Proceedings of the First Joint Eurohaptics Conference and Symposium on Haptic Interfaces for Virtual Environment and Teleoperator Systems, 2005.

[8] D. Xiao, R. Hubbold, Navigation guided by artificial force fields, in: Proceedings of ACM CHI 98 Conference on Human Factors in Computing Systems, Vol. 1, 1998, pp. 179–186.

[9] R. Hubbold, M. Keates, Real-time simulation of a stretcher evacuation in a large-scale virtual environment, Computer Graphics Forum 19 (2).

[10] M. A. Otaduy, M. C. Lin, Stable and Responsive Six-Degree-of-Freedom Haptic Manipulation Using Implicit Integration, in: Proceedings of the First Joint Eurohaptics Conference and Symposium on Haptic Interfaces for Virtual Environment and Teleoperator Systems, 2005.

[11] J. Martín, J. Savall, Mechanisms for Haptic Torque Feedback, in: Proceedings of the First Joint Eurohaptics Conference and Symposium on Haptic Interfaces for Virtual Environment and Teleoperator Systems, 2005.

[12] M. A. Otaduy, M. C. Lin, Sensation preserving simplification for haptic rendering, ACM SIGGRAPH 2003 / ACM Transactions on Graphics 22 (2003) 543–553.

[13] C. Richard, M. R. Cutkosky, Friction Identification for Haptic Display, in: Proceedings of the 1999 ASME IMECE, 1999.

[14] H. Iwata, H. Yano, R. Kawamura, Array Force Display for Hardness Distribution, in: Proceedings of the 10th International Symposium on Haptic Interfaces for Virtual Environments and Teleoperator Systems (HAPTICS'02), 2002.

[15] J. Zhang, S. Payandeh, J. Dill, Haptic Subdivision: an Approach to Defining Level-of-detail in Haptic Rendering, in: Proceedings of the 10th International Symposium on Haptic Interfaces for Virtual Environments and Teleoperator Systems (HAPTICS'02), 2002.

[16] M. Mahvash, V. Hayward, High-Fidelity Haptic Synthesis of Contact with Deformable Bodies, IEEE Computer Graphics and Applications (2004) 48–55.

[17] E. Vidholm, I. Nyström, A haptic interaction technique for volume images based on gradient diffusion, in: Proceedings of the First Joint Eurohaptics Conference and Symposium on Haptic Interfaces for Virtual Environment and Teleoperator Systems, 2005.

[18] K. S. Hale, K. M. Stanney, Deriving haptic design guidelines from human physiological, psychophysical, and neurological foundations, IEEE Computer Graphics and Applications (2004) 33–39.

[19] A. Gregory, M. Lin, S. Gottschalk, R. Taylor., H-collide: A framework for fast and accurate collision detection for haptic interaction, in: Proceedings of IEEE Virtual Reality Conference 1999, IEEE, 1999, p. 38Ð45.

[20] D. E. Johnson, P. Willemsen, Accelerated Haptic Rendering of Polygonal Models through Local Descent, in: Proceedings of the 12th International Symposium on Haptic Interfaces for Virtual Environment and Teleoperator Systems (HAPTICS?04), 2004.

[21] H. B. Morgenbesser, M. A. Srinivasan, Force shading for haptic shape perception, in: Proceedings of the ASME Intl Mechanical Eng. Congress and Exposition, Dynamic Systems and Control Division, 1996, pp. 407–412.

[22] M. Minsky, S. Lederman, Simulated haptic textures: Roughness, in: Proceedings of the ASME Dynamic Systems and Control Division, Vol. 58, 1996.

[23] J. Siira, D. K. Pai, Haptic texturing: A stochastic approach, in: IEEE International Conference on Robotics and Automation, Vol. 1, 1996.

[24] M. A. Costa, M. R. Cutkosky, Roughness perception of haptically displayed fractal surfaces, in: Proceedings of the ASME Dynamic Systems and Control Division, Vol. 69, 2000.

[25] R. Klatzky, S. Lederman, Touch in Virtual Environments, Prentice-Hall PTR, 2002, Ch. Perceiving Texture through a Probe (Chapter 10).

[26] A. Watt, M. Watt, Advanced animation and rendering techniques, ACM Press, New York, NY, USA, 1991.

[27] C.-H. Ho, C. Basdogan, M. A. Srinivasan, Efficient point-based rendering techniques for haptic display of virtual objects, Presence 8 (5) (1999) 477–491.

[28] R. Jagnow, J. Dorsey, Virtual sculpting with haptic displacement maps, in: Graphics Interface'02), 2002, pp. 125–132.

[29] S. Choi, H. Z. Tan, Perceived instability of virtualhaptic texture. i. experimental studies, Presence 13 (4).

[30] S. Choi, H. Z. Tan, Perceived instability of virtualhaptic texture. ii. effect of collision-detection algorithm, Presence 14 (4).

[31] L. Kim, G. S. Sukhatme, M. Desbrun, A haptic-rendering technique based on hybrid surface representation, IEEE Computer Graphics and Applications (2004) 66–75.

[32] K. Potter, D. Johnson, E. Cohen, Height Field Haptics, in: Proceedings of the 12th International Symposium on Haptic Interfaces for Virtual Environment and Teleoperator Systems (HAPTICS?04), 2004.

[33] M. Otaduy, N. Jain, A. Sud, M. Lin, Haptic display of interaction between textured models, in: IEEE Visualization 2004, 2004, pp. 297–304.

[34] S. D. Laycock, A. M. Day, A survey of haptic rendering techniques, COMPUTER GRAPHICS forum 26 (1) (2007) 50–65.

[35] J. F. Blinn, Simulation of wrinkled surfaces, in: Proceedings of SIGGRAPH'78, ACM, 1978.

[36] V. Theoktisto, M. Fairén, I. Navazo, E. Monclús, Rendering detailed haptic textures, in: Proceedings of Second Workshop in Virtual Reality Interactions and Physical Simulations (VRIPHYS '05), Pisa, Italy, 2005.

[37] J. Shankel, Fast Heightfield Normal Calculation, in: Game Programming Gems 3, Charles River Media, Inc., 2002, pp. 344–348.

[38] C. Bosch, X. Pueyo, S. Mérillau, D. Ghazanfarpour, A physically-based model for rendering realistic scratches, Computer Graphics Forum 23 (3).

[39] F. Policarpo, M. M. Oliveira, J. L. D. Comba, Real-time relief mapping on arbitrary polygonal surfaces, in: SI3D '05: Proceedings of the 2005 symposium on Interactive 3D graphics and games, ACM Press, New York, NY, USA, 2005, pp. 155–162.

[40] L. Baboud, X. Décoret, Rendering geometry with relief textures, in: Graphics Interface '06, Quebec, Canada, 2006.